



**AFRL-RX-WP-JA-2015-0162**

**AN EBSD INVESTIGATION OF CRYOGENICALLY-ROLLED CU-30%ZN BRASS (POSTPRINT)**

**S. L. Semiatin**  
**Air Force Research Laboratory**

**T. Konkova and G. Korznikova**  
**Institute for Metals Superplasticity Problems, Russian Academy of Science**

**S. Mironov**  
**Department of Materials Processing, Graduate School of Engineering,**  
**Tohoku University**

**A. Korznikov**  
**National Research Tomsk State University**

**M. M. Myshlyaev**  
**Baikov Institute of Metallurgy and Material Science, Russian Academy of Science**

**MARCH 2015**  
**Interim Report**

**Distribution Statement A. Approved for public release; distribution unlimited.**

*See additional restrictions described on inside pages*

**STINFO COPY**

**© 2015 Elsevier, Inc.**

**AIR FORCE RESEARCH LABORATORY**  
**MATERIALS AND MANUFACTURING DIRECTORATE**  
**WRIGHT-PATTERSON AIR FORCE BASE OH 45433-7750**  
**AIR FORCE MATERIEL COMMAND**  
**UNITED STATES AIR FORCE**

## NOTICE AND SIGNATURE PAGE

Using Government drawings, specifications, or other data included in this document for any purpose other than Government procurement does not in any way obligate the U.S. Government. The fact that the Government formulated or supplied the drawings, specifications, or other data does not license the holder or any other person or corporation; or convey any rights or permission to manufacture, use, or sell any patented invention that may relate to them.

Qualified requestors may obtain copies of this report from the Defense Technical Information Center (DTIC) (<http://www.dtic.mil>).

AFRL-RX-WP-JA-2015-0162 HAS BEEN REVIEWED AND IS APPROVED FOR PUBLICATION IN ACCORDANCE WITH ASSIGNED DISTRIBUTION STATEMENT.

//Signature//

---

S. L. SEMIATIN, Project Engineer  
Metals Branch  
Structural Materials Division

//Signature//

---

DANIEL J. EVANS, Chief  
Metals Branch  
Structural Materials Division

//Signature//

---

ROBERT T. MARSHALL, Deputy Chief  
Structural Materials Division  
Materials And Manufacturing Directorate

This report is published in the interest of scientific and technical information exchange and its publication does not constitute the Government's approval or disapproval of its ideas or findings.

# REPORT DOCUMENTATION PAGE

Form Approved  
OMB No. 0704-0188

The public reporting burden for this collection of information is estimated to average 1 hour per response, including the time for reviewing instructions, searching existing data sources, gathering and maintaining the data needed, and completing and reviewing the collection of information. Send comments regarding this burden estimate or any other aspect of this collection of information, including suggestions for reducing this burden, to Department of Defense, Washington Headquarters Services, Directorate for Information Operations and Reports (0704-0188), 1215 Jefferson Davis Highway, Suite 1204, Arlington, VA 22202-4302. Respondents should be aware that notwithstanding any other provision of law, no person shall be subject to any penalty for failing to comply with a collection of information if it does not display a currently valid OMB control number. **PLEASE DO NOT RETURN YOUR FORM TO THE ABOVE ADDRESS.**

<b>1. REPORT DATE (DD-MM-YY)</b> March 2015			<b>2. REPORT TYPE</b> Interim		<b>3. DATES COVERED (From - To)</b> 19 March 2014 – 4 February 2015	
<b>4. TITLE AND SUBTITLE</b> AN EBSD INVESTIGATION OF CRYOGENICALLY-ROLLED CU-30%ZN BRASS (POSTPRINT)					<b>5a. CONTRACT NUMBER</b> In-house	
					<b>5b. GRANT NUMBER</b>	
					<b>5c. PROGRAM ELEMENT NUMBER</b> 62102F	
<b>6. AUTHOR(S)</b> See back.					<b>5d. PROJECT NUMBER</b> 4349	
					<b>5e. TASK NUMBER</b>	
					<b>5f. WORK UNIT NUMBER</b> X0W6	
<b>7. PERFORMING ORGANIZATION NAME(S) AND ADDRESS(ES)</b>  See back.					<b>8. PERFORMING ORGANIZATION REPORT NUMBER</b>	
<b>9. SPONSORING/MONITORING AGENCY NAME(S) AND ADDRESS(ES)</b>  Air Force Research Laboratory Materials and Manufacturing Directorate Wright-Patterson Air Force Base, OH 45433-7750 Air Force Materiel Command United States Air Force					<b>10. SPONSORING/MONITORING AGENCY ACRONYM(S)</b> AFRL/RXC	
					<b>11. SPONSORING/MONITORING AGENCY REPORT NUMBER(S)</b> AFRL-RX-WP-JA-2015-0162	
<b>12. DISTRIBUTION/AVAILABILITY STATEMENT</b> Distribution Statement A. Approved for public release; distribution unlimited.						
<b>13. SUPPLEMENTARY NOTES</b> PA Case Number: 88ABW-2014-3995, Clearance Date: 26 August 2014. Journal article published in <i>Materials Characterization</i> 101, (2015), 173-179. © 2015 Elsevier, Inc. The U.S. Government is joint author of the work and has the right to use, modify, reproduce, release, perform, display or disclose the work. This report contains color. The final publication is available at <a href="http://dx.doi.org/10.1016/j.matchar.2015.02.004">http://dx.doi.org/10.1016/j.matchar.2015.02.004</a> .						
<b>14. ABSTRACT</b> Electron backscatter diffraction was used to study grain structure development in heavily cryogenically-rolled Cu-30%Zn brass. The produced microstructure was found to be very inhomogeneous. At a relatively coarse scale, it consisted of texture bands having crystallographic orientations close to the $\alpha$ - and $\gamma$ -fibers. The texture bands contained internal structure comprising shear bands, mechanical twins, and low-angle boundaries. Such features were more pronounced within the $\gamma$ -fiber, and this resulted in a heterogeneous ultrafine grain structure. The cryogenic rolling was concluded to be not straightforward for production of nanocrystalline grain structure in Cu-30%Zn brass.						
<b>15. SUBJECT TERMS</b> Cu-30Zn brass, grain refinement, cryogenic deformation, electron backscatter diffraction, grain structure, texture						
<b>16. SECURITY CLASSIFICATION OF:</b>			<b>17. LIMITATION OF ABSTRACT:</b>  SAR	<b>18. NUMBER OF PAGES</b>  11	<b>19a. NAME OF RESPONSIBLE PERSON (Monitor)</b> S. L. Semiatin <b>19b. TELEPHONE NUMBER (Include Area Code)</b> (937) 255-1345	
<b>a. REPORT</b>  Unclassified	<b>b. ABSTRACT</b>  Unclassified	<b>c. THIS PAGE</b>  Unclassified				

## REPORT DOCUMENTATION PAGE Cont'd

### 6. AUTHOR(S)

S. L. Semiatin - Materials and Manufacturing Directorate, Air Force Research Laboratory

T. Konkova and G. Korznikova - Institute for Metals Superplasticity Problems, Russian Academy of Science

S. Mironov - Department of Materials Processing, Graduate School of Engineering, Tohoku University

A. Korznikov - National Research Tomsk State University

M. M. Myshlyayev - Baikov Institute of Metallurgy and Material Science, Russian Academy of Science

### 7. PERFORMING ORGANIZATION NAME(S) AND ADDRESS(ES)

Air Force Research Laboratory  
Materials and Manufacturing Directorate  
Wright-Patterson AFB, OH 45433

Institute for Metals Superplasticity Problems  
Russian Academy of Science  
39 Khalturin Str., Ufa 450001, Russia

Department of Materials Processing  
Graduate School of Engineering  
Tohoku University  
6-6-02 Aramaki-aza-Aoba  
Sendai 980-8579, Japan

National Research Tomsk State University  
36 Lenina av.  
Tomsk 634050, Russia

Baikov Institute of Metallurgy and Material Science  
Russian Academy of Science  
49 Lenin-av.  
Moscow 119991, Russia



# An EBSD investigation of cryogenically-rolled Cu–30%Zn brass



T. Konkova<sup>a</sup>, S. Mironov<sup>a,b,\*</sup>, A. Korznikov<sup>a,c</sup>, G. Korznikova<sup>a</sup>, M.M. Myshlyaev<sup>d</sup>, S.L. Semiatin<sup>e</sup>

<sup>a</sup> Institute for Metals Superplasticity Problems, Russian Academy of Science, 39 Khalturin Str., Ufa 450001, Russia

<sup>b</sup> Department of Materials Processing, Graduate School of Engineering, Tohoku University, 6-6-02 Aramaki-aza-Aoba, Sendai 980-8579, Japan

<sup>c</sup> National Research Tomsk State University, 36 Lenina av., Tomsk 634050, Russia

<sup>d</sup> Baikov Institute of Metallurgy and Material Science, Russian Academy of Science, 49 Lenin-av., Moscow 119991, Russia

<sup>e</sup> Air Force Research Laboratory, Materials and Manufacturing Directorate, AFRL/RXCM, Wright-Patterson AFB, OH 45433-7817, USA

## ARTICLE INFO

### Article history:

Received 8 August 2014

Received in revised form 30 January 2015

Accepted 4 February 2015

Available online 7 February 2015

### Keywords:

Cu–30Zn brass

Grain refinement

Cryogenic deformation

Electron backscatter diffraction

Grain structure

Texture

## ABSTRACT

Electron backscatter diffraction was used to study grain structure development in heavily cryogenically rolled Cu–30%Zn brass. The produced microstructure was found to be very inhomogeneous. At a relatively coarse scale, it consisted of texture bands having crystallographic orientations close to the  $\alpha$  and  $\gamma$  fibers. The texture bands contained internal structure comprising shear bands, mechanical twins, and low angle boundaries. Such features were more pronounced within the  $\gamma$  fiber, and this resulted in a heterogeneous ultrafine grain structure. The cryogenic rolling was concluded to be not straightforward for production of nanocrystalline grain structure in Cu–30%Zn brass.

© 2015 Elsevier Inc. All rights reserved.

## 1. Introduction

The possibility of a substantial improvement in the mechanical properties of alloys has given rise to considerable commercial interest in techniques for grain refinement. Of particular importance are cost effective methods that can be used for production of large quantities of ultrafine grain materials. In this regard, an approach involving large deformation at cryogenic temperatures has recently attracted significant attention. It is believed that low temperatures may suppress dynamic recovery and stimulate mechanical twinning, thereby enhancing the grain refinement effect. This may decrease the level of strain necessary to achieve an ultrafine microstructure and thus enable the application of conventional working processes such as rolling to obtain such materials.

To date, the majority of research in the field of cryogenic working has focused on aluminum alloys and pure copper [e.g., 1–7]. In both materials, cryogenic rolling has been found to provide no significant grain refinement effect [1,2]. This disappointing observation has been attributed to the suppression of cross slip under cryogenic conditions, thus leading to a retardation of the formation of dislocation boundaries [2]. On the other hand, pronounced microstructural refinement has been observed during *dynamic* (high strain rate) cryogenic deformation

of copper [3] and alpha brass [8] as well as during cryogenic rolling of commercial purity titanium [9]. In all cases, the formation of an ultrafine grain structure has been attributed to mechanical twinning and shear banding. Thus, it appears that cryogenic deformation is most effective for materials prone to activation of these two deformation mechanisms.

Due to its very low stacking fault energy, extensive twinning and shear banding usually occur during cold deformation of Cu–30Zn brass, and thus significant grain refinement may be expected. This effect is well documented for rolling of this material at ambient temperature [10], as well as for dynamic cryogenic deformation [8], as mentioned above. Because dislocations in this alloy are dissociated into partials, a distinct cell structure is not formed. This gives rise to significant strain hardening and the activation of profuse mechanical twinning after a true strain of ~0.6 [8,10]. The extensive twinning produces a nanoscale, lamellar like, twin matrix structure. Due to the very small slip distance, subsequent slip in the twinned areas occurs primarily along a common twin/matrix {111} plane [10]. This provides a rotation of the slip plane toward the rolling plane, thus reducing the associated Schmid factor for slip to zero [10]. As a result of the suppression of grain scale slip, intense shear banding occurs after true strains of ~0.8 [8,10]. This eventually leads to the formation of a nanoscale structure [8,10].

It should be noted that prior microstructural observations of heavily cold rolled alpha brass were performed primarily by transmission electron microscopy (TEM). Despite the excellent resolution of TEM, the statistical reliability of such results is not clear. Hence, the objective

\* Corresponding author at: Department of Materials Processing, Graduate School of Engineering, Tohoku University, 6-6-02 Aramaki-aza-Aoba, Sendai 980-8579, Japan.

E-mail address: [smironov@material.tohoku.ac.jp](mailto:smironov@material.tohoku.ac.jp) (S. Mironov).



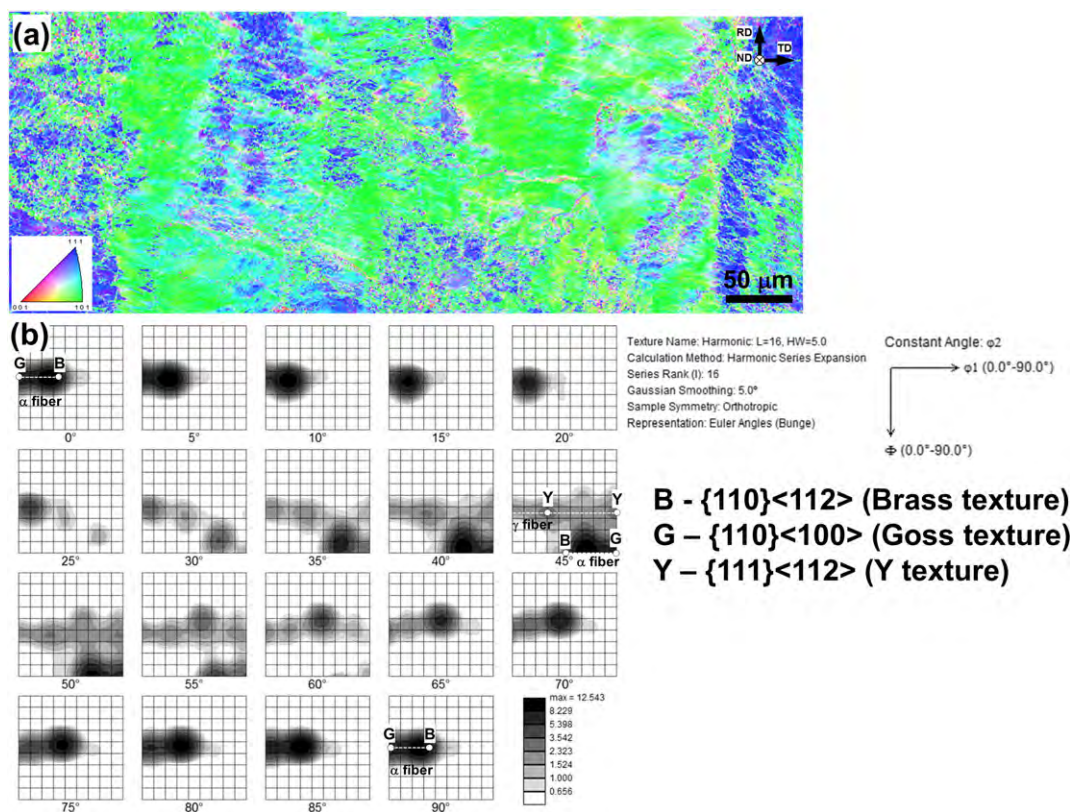


**Fig. 1.** Texture of cryo-rolled brass: (a) Low-resolution EBSD inverse-pole-figure map (color orientation code is shown in the bottom left corner), (b) orientation distribution function derived from the map. In (b), some of the ideal rolling textures for face-centered cubic metals [12] are also shown.

of the present work was to provide deeper insight into the mechanisms of grain refinement and texture evolution during cryogenic rolling of Cu 30%Zn brass using electron back scatter diffraction (EBSD) imaging.

## 2. Materials and methods

The program material comprised Cu 30%Zn, variously referred to as yellow or cartridge brass, with a measured composition (in wt.%) of 29.5 Zn, 0.5 Pb and balance Cu. It was manufactured by ingot casting followed by 10% cold rolling and subsequent annealing at 800 °C for 30 min. This processing route produced millimeter size grains which retained some degree of the original dendritic structure, but very few annealing twins.

The material was cryogenically rolled to 90 pct. overall thickness reduction (true strain = −2.3) using a reduction per pass of 10 pct. In order to provide cryogenic deformation conditions, the rolling preform and work rolls were soaked in liquid nitrogen prior to each pass and held for 20 min; immediately after each pass, the workpiece was re inserted into liquid nitrogen. The typical flat rolling convention was adopted in this work; i.e., the rolling, long transverse, and thickness/normal directions were denoted as RD, TD, and ND, respectively.

To preserve the deformation induced microstructure, the cryo rolled material was stored in a freezer at ~−20 °C prior to examination.

Microstructure characterization was performed primarily via EBSD examination of the mid thickness rolling plane (containing the RD and TD). For this purpose, samples were prepared using conventional metallographic techniques followed by long term (24 h) vibratory polishing with a colloidal silica suspension. EBSD analysis was conducted with a JSM 7800F field emission gun, scanning electron microscope equipped with a TSL OIM™ EBSD system. To examine microstructure at different scales, several EBSD maps were acquired with a scan step size of 0.05 or 0.25 μm. To differentiate the maps, they are denoted as “high resolution” and “low resolution”, respectively, throughout this paper. To

improve the reliability of the EBSD data, small grains comprising three or fewer pixels were automatically removed from the maps using the grain dilation option in the TSL software; this procedure thus excluded grains smaller than ~0.09 μm from consideration. Furthermore, to eliminate spurious boundaries caused by orientation noise, a lower limit boundary misorientation cutoff of 2° was used. A 15° criterion was employed to differentiate low angle boundaries (LABs) and high angle boundaries (HABs). Grain size was quantified by the determination of the area of each grain and the calculation of its circle equivalent diameter, i.e., the so called grain reconstruction method was applied [11].

## 3. Results and discussion

The principal results of this work comprised quantitative determination of various texture and microstructure features.

### 3.1. Texture

A composite<sup>1</sup> low resolution EBSD inverse pole figure (IPF) map for the cryo rolled material is shown in Fig. 1a; in the map, individual grains are colored according to their crystallographic directions relative to the ND using the typical color code triangle in the bottom left corner of the figure.<sup>2</sup> From a broad perspective, the structure consisted of bands aligned with the RD and having a crystallographic orientation close to <110>//ND or <111>//ND (green and blue colors, respectively).

<sup>1</sup> Note: EBSD maps shown in Figs. 1a & 3 were obtained by stitching two smaller EBSD maps.

<sup>2</sup> Here and hereafter, a reader is referred to on-line version of the paper to see figures in color.

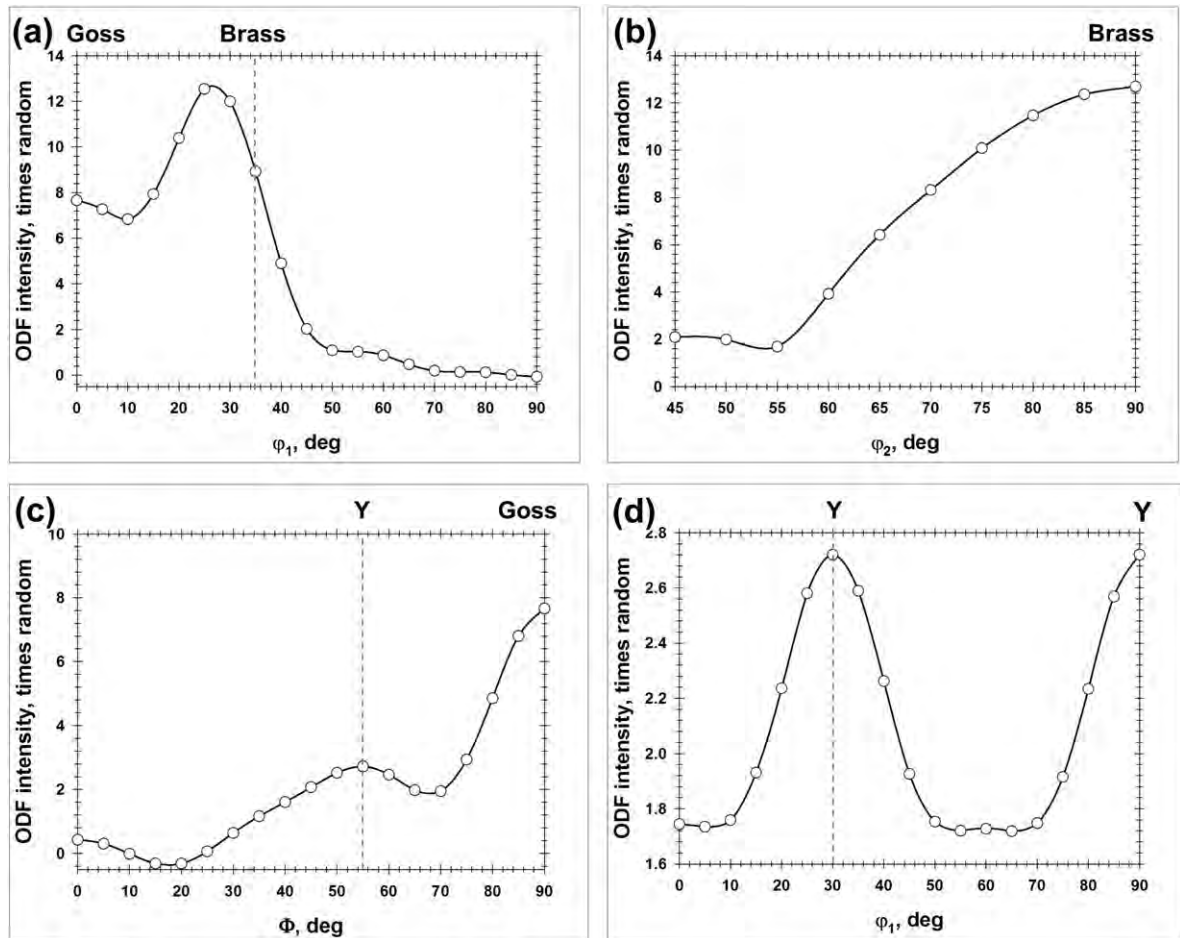


Fig. 2. Distribution of texture intensity (x random) along (a)  $\alpha$ -fiber, (b)  $\beta$ -fiber, (c)  $\tau$ -fiber, and (d)  $\gamma$ -fiber.

Orientation data from the IPF map were used to quantify the crystallography of the banded structure in more detail (Figs. 1b, 2 and Table 1). For comparison purposes, several ideal rolling orientations for face centered cubic metals (after Hirsch, et al. [12]) are shown in Fig. 1b. To a first approximation, the observed texture was interpreted in terms of the superposition of two partial fibers  $\alpha <110>/\text{ND}$  and  $\gamma <111>/\text{ND}$  (Figs. 1b and 2); the  $\alpha$  fiber was more pronounced than the  $\gamma$  fiber (Table 1). Thus, the texture bands in Fig. 1a are indicative of the  $\alpha$  and  $\gamma$  fibers. Within the  $\alpha$  fiber, strong Brass  $\{110\}<112>$  and Goss  $\{110\}<100>$  components were noted (Figs. 1b & 2a), whereas the  $\gamma$  fiber was dominated by the Y  $\{111\}<112>$  texture component (Figs. 1b & 2d). The Brass, Goss and Y components were characterized by large orientation spreads which gave rise to texture intensity along the  $\beta$  and  $\tau$  fibers (Fig. 2b & c). Furthermore, the Brass orientation was

found to be shifted from the expected  $\phi_1 = 35^\circ$  location toward  $\phi_1 = 25^\circ$  (Fig. 2a), i.e., from  $\{110\}<112>$  to  $\{110\}<113>$ . The reason for this effect is unclear.

The measured texture was as expected for heavily cold rolled brass [10]. The Brass component is commonly accepted to be a stable end orientation, whereas Y and Goss are typically transient orientations originating from twinning, slip, and subsequent shear banding [10]. The origin of the latter two orientations is discussed in more detail in Section 3.3.

### 3.2. Microstructure

Insight into grain structure evolution was obtained from Kikuchi band (image quality) and grain boundary maps (Fig. 3) which were

Table 1  
Volume fractions of texture components.

Texture component		Volume fraction (pct.) within 15-deg. tolerance
Notation	Crystallographic orientation	
$\alpha$ -Fiber	$<110>/\text{ND}$	49.0
$\gamma$ -Fiber	$<111>/\text{ND}$	17.4
Brass	$\{110\}<112>/\{110\}<113>$	22.5/30.8
Goss	$\{110\}<100>$	9.9
Y	$\{111\}<112>$	7.3

\*Note: Predominant orientations are highlighted in gray.



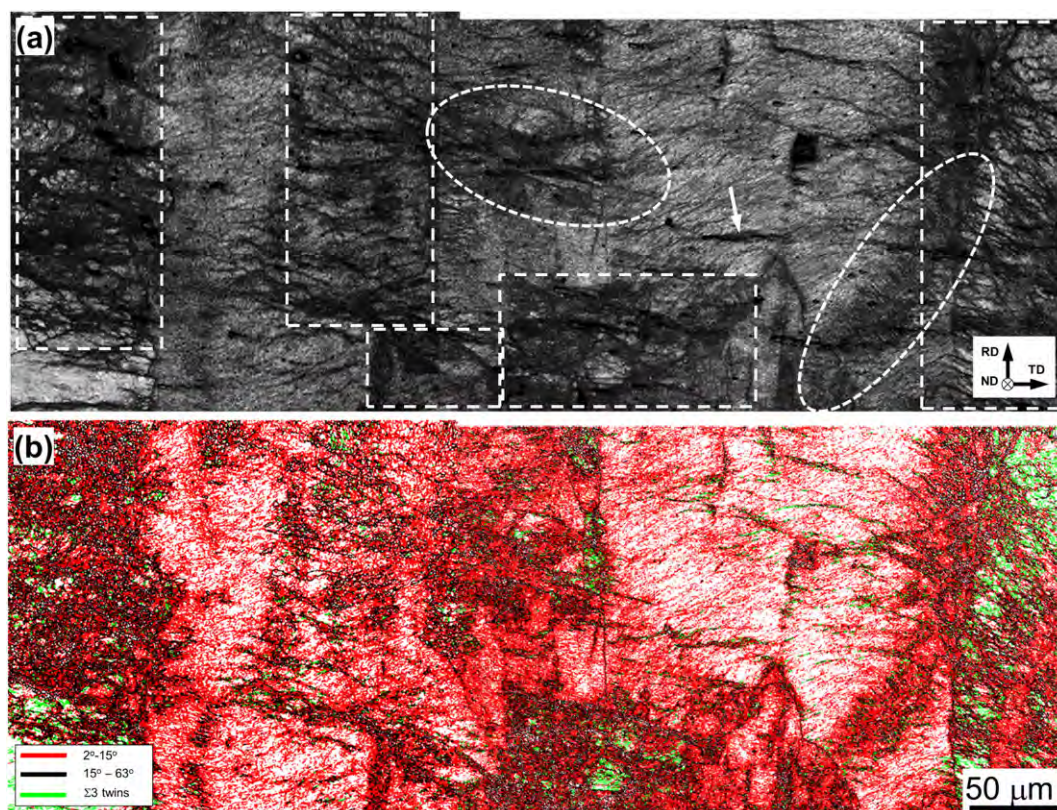


Fig. 3. Low resolution EBSD maps illustrating grain structure of cryo-rolled brass: (a) Kikuchi-band map and (b) grain-boundary map. In (a), selected areas show clustering of deformation bands.

derived from the same region as the IPF map in Fig. 1a. Of particular interest were dark bands in the image contrast map such as that indicated by an arrow in Fig. 3a. As shown below, these bands comprised an ultrafine grain structure, thus likely being shear bands commonly observed in heavily cold rolled brass. Importantly, the shear bands were preferentially concentrated within the  $\gamma$  fiber as deduced by a comparison of Figs. 1a and 3a. Moreover, the  $\gamma$  fiber was also characterized by a larger twin content and denser LAB substructure than found in the  $\alpha$  fiber (Figs. 3b & 1a).

Higher resolution EBSD data within the specific texture bands provided a clearer view of the substructure within the  $\alpha$  and  $\gamma$  fibers (Figs. 4 and 5). Within the  $\alpha$  fiber, shear bands were observed only sporadically (arrows in Fig. 4a). They were characterized by a very fine grain structure and were surrounded by twins (Fig. 4b). Interestingly, the shear bands lay relatively close to traces of  $\{111\}$

close packed planes (Fig. 4a). All these observations agree well with those for shear bands found in alpha brass heavily rolled at room temperature [10]. With the exception of the shear bands, the substructure of the  $\alpha$  fiber was relatively simple. It was dominated by nearly parallel arrays of LABs which were aligned with the  $\{111\}$  plane traces (Fig. 4b). Such lamellar substructures are typical for heavily cold rolled cubic metals, and are usually attributed to a specific grain subdivision mechanism [13]. The observed lamellar boundaries were typically low angle in nature (Fig. 4b) thus indicating that the LAB to HAB transformation was relatively slow. In addition, very fine, equiaxed grains were observed sporadically in the microstructure (an example is circled in Fig. 4b); their origin is not clear.

The substructure within the  $\gamma$  fiber, by contrast, was more complicated, mainly as a result of numerous shear bands and series of

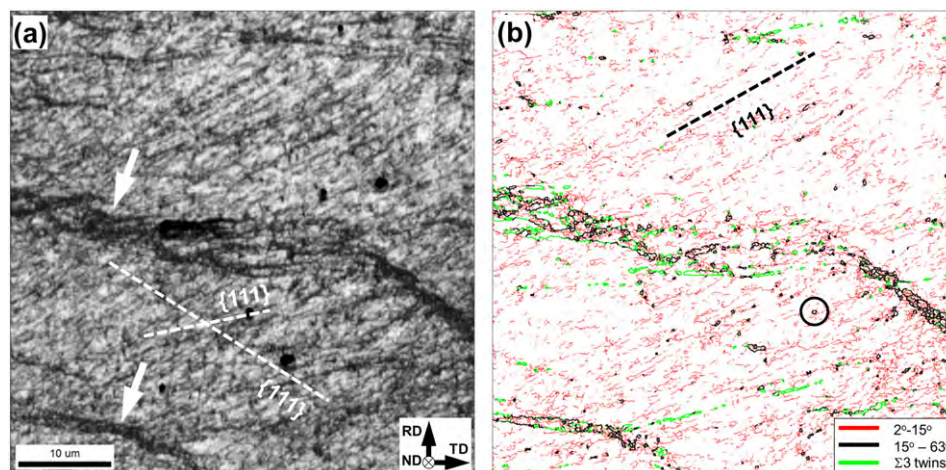
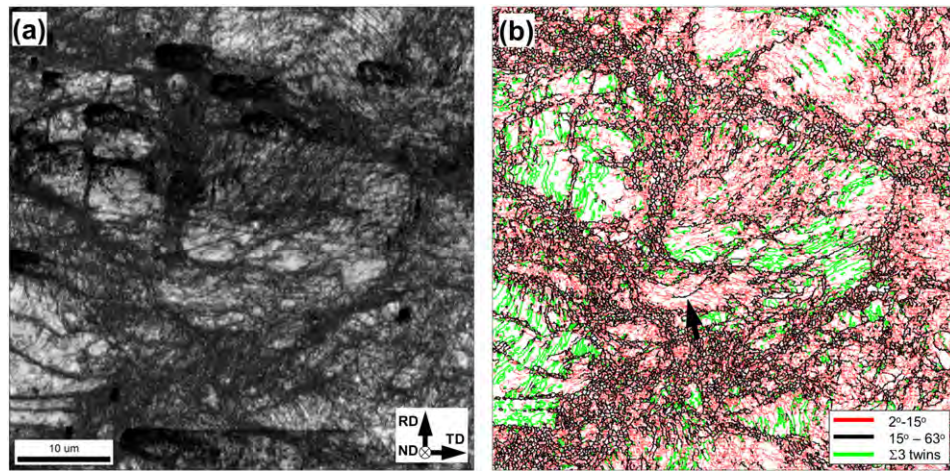
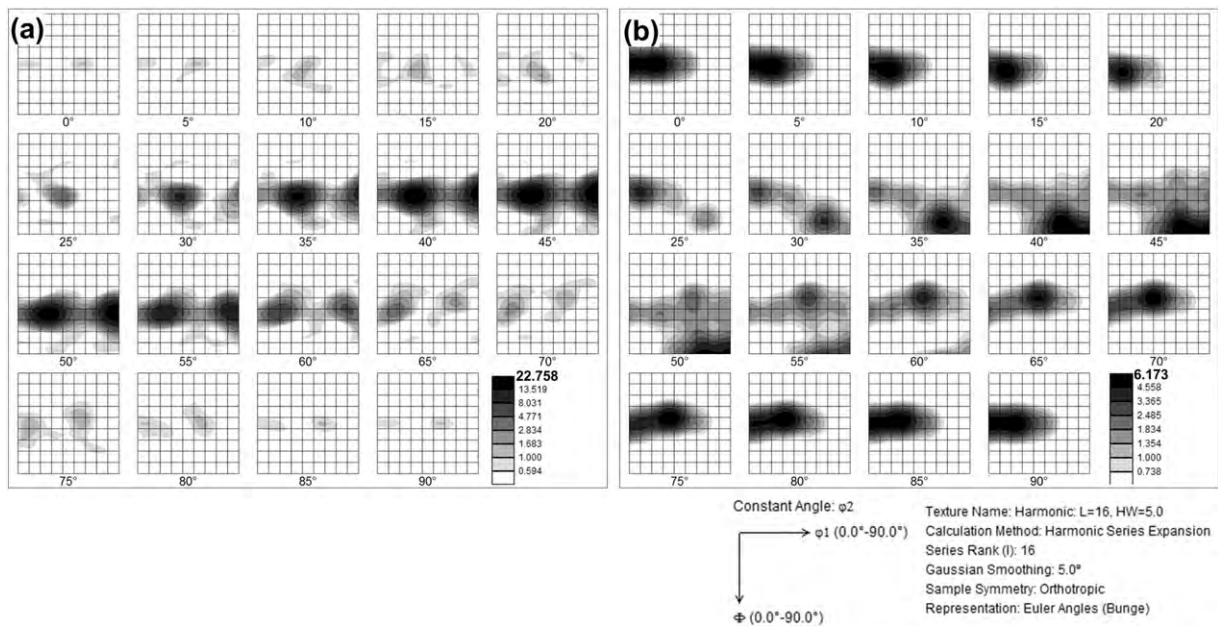


Fig. 4. Microstructure within the  $\alpha$ -fiber bands: (a) Image-quality map and (b) grain-boundary map. In (a), arrows indicate deformation bands; broken lines indicate traces of  $\{111\}$  planes.





**Fig. 5.** Microstructure within the  $\gamma$ -fiber bands: (a) Image-quality map and (b) grain-boundary map. In (b), the arrow indicates an example of a deformation-induced HAB.



**Fig. 6.** Orientation distribution functions showing texture within (a) twinned areas and (b) shear bands.

twins (Fig. 5). The mean grain size within the shear bands was  $\sim 0.2 \mu\text{m}$ . The twins had nearly lenticular morphology and were also  $\sim 0.2 \mu\text{m}$  in thickness (Fig. 5b) thus providing evidence of their deformation origin. The LAB substructure was relatively dense and complicated, but the lamellar morphology seemed to predominate (Fig. 5b). The mean LAB misorientation was higher than that in the  $\alpha$  fiber ( $5.8^\circ$  vs  $4.4^\circ$ ), thus suggesting more rapid microstructural evolution in the  $\gamma$  fiber. Some subboundary segments even accumulated misorientations over  $15^\circ$ , thus transforming into deformation induced HABs; an example is indicated by the arrow in Fig. 5b. However, such transformations were relatively rare, and thus grain refinement within the  $\gamma$  fiber was largely a result of shear banding and twinning (Fig. 5b).

It is worth noting that the grain structure revealed in the present study is substantially coarser than those observed by Xiao et al. in dynamically cryo deformed brass [8]. In the earlier work, the formation of nanoscale microstructure consisting of  $\sim 50 \text{ nm}$  grains within shear bands and  $\sim 10 \text{ nm}$  twins was reported [8]. This discrepancy may be related to different deformation conditions (i.e., rolling vs dynamic plastic deformation) or different microstructure characterization techniques (EBSD vs TEM) used in these efforts.

### 3.3. Crystallographic orientations of twinned areas and shear bands

Due to the large impact of twinning and shear banding on grain refinement, their origin was of particular interest. Thus, the crystallographic orientations of these features were extracted from EBSD maps and are summarized in Figs. 6 & 7 and Table 2.

The crystallographic orientations of the twinned areas were close to the  $\gamma$  fiber (Fig. 6a, Table 2) with a pronounced Y  $\{111\}$ - $\langle 112 \rangle$  texture component (Figs. 6a & 7d, Table 2). This is as expected for heavily cold rolled brass. The Y texture is commonly accepted to originate from mechanical twinning of grains with the Copper  $\{112\}$ - $\langle 111 \rangle$  orientation, which occurs at an intermediate level of rolling reduction, and the subsequent slip of the twinned and matrix material on the common  $\{111\}$  twinning plane [10].

The orientation distribution of the shear bands was more complex. It included elements of the  $\alpha$  fiber<sup>3</sup> with strong Brass and Goss components

<sup>3</sup> Spatially, the shear bands were preferentially located within the  $\gamma$  texture bands (Fig. 1a). However, their crystallographic orientations were often close to the  $\alpha$  fiber (Fig. 6b). Thus, shear banding was associated with the transformation of the  $\gamma$  fiber into the  $\alpha$  fiber.

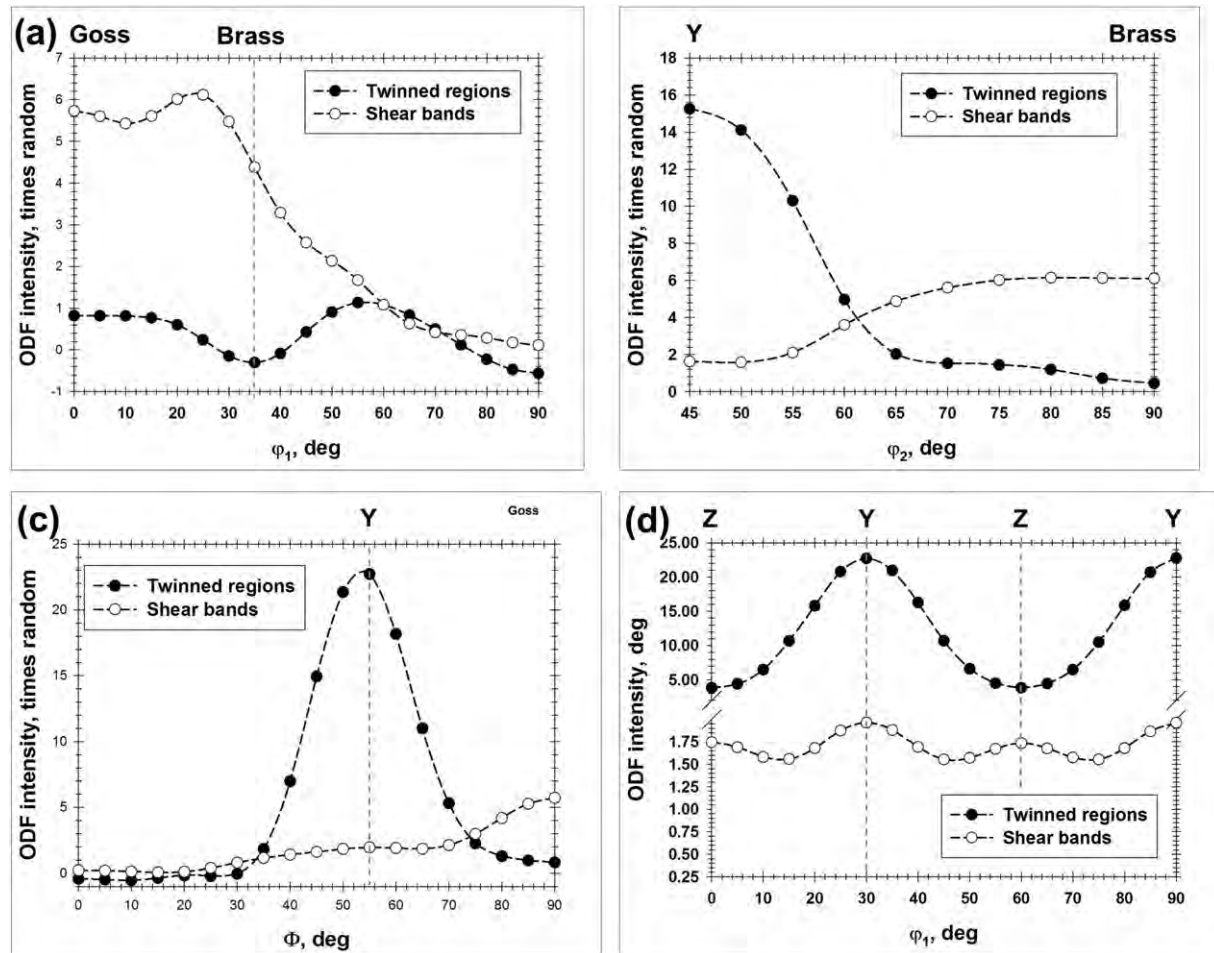


Fig. 7. Intensity (x random) of twinned-region and shear-band texture components within (a)  $\alpha$ -fiber, (b)  $\beta$ -fiber, (c)  $\tau$ -fiber, and (d)  $\gamma$ -fiber.

(Figs. 6b & 7a, Table 2) as well as the  $\gamma$  fiber (Fig. 6b) with Y and Z  $\{111\}<110>$  orientations (Fig. 7d, Table 2). All of these observations are in line with the typical textures developed during rolling of brass at room temperature [10]. The Z orientation is believed to originate from twinning of the S  $\{123\}<634>$  component (developed at moderate rolling reductions) and subsequent slip. Together with the Copper twins, this produces the  $\gamma$  fiber. This fiber consists of packages of very narrow ( $\sim 0.1 \mu\text{m}$ ) twin/matrix lamellae and is characterized by an alignment of  $\{111\}$  planes with the rolling plane. In the  $\gamma$  fiber, the further slip is believed to be increasingly difficult because either the Schmid factor for

slip on the operative plane decreases toward zero or the slip distance for slip on the other  $\{111\}$  planes is limited. Such geometrically strengthened structures are believed to be highly unstable and prone to shear banding. The shear bands rotate the  $\gamma$  fiber toward the Goss orientation, and subsequent slip in the Goss produces the final stable Brass texture. The presence of the Y, Z, Goss, and Brass orientations within the shear bands revealed in this work thus reflect different stages of texture development.

It is also noteworthy that the peak intensity of the orientation distribution of the shear bands was relatively low (Fig. 6b). This observation

Table 2

Volume fractions of texture components in twinned regions and within shear bands.

Texture component		Volume fraction (pct.) within 15-deg. tolerance	
Notation	Crystallographic orientation	Twinned region	Shear bands
$\alpha$ -Fiber	$\langle 110 \rangle // \text{ND}$	7.4	32.0
$\gamma$ -Fiber	$\langle 111 \rangle // \text{ND}$	76.0	13.5
Brass	$\{110\}\langle 112 \rangle / \{110\}\langle 113 \rangle$	1.8/1.5	11.5/14.8
Goss	$\{110\}\langle 100 \rangle$	1.5	6.6
Y	$\{111\}\langle 112 \rangle$	50.6	4.7
Z	$\{111\}\langle 110 \rangle$	12.8	5.3

\*Note: Predominant orientations are highlighted in gray.

is consistent with the large orientation spread typically found within shear bands in cold rolled brass [10], and can be attributed to the complex character of slip within the shear bands.

From the above results, it appears that the twinning and shear banding processes at cryogenic temperatures are broadly similar to those occurring during rolling at room temperature. Therefore, grain refinement during cryogenic rolling should also be governed by the development of the easily twinned Copper and S orientations at intermediate levels of strain. To increase the volume fraction of the fine grained structure in the final material, it is thus necessary to promote the extensive formation of the Copper and S orientations at moderate levels of reduction. Unfortunately, it is not clear now how this can be achieved.

It is also worth noting that a benefit of rolling at cryogenic temperature to refine the grain size was not evident. To clarify this issue, a direct comparison of microstructures produced by conventional cold rolling and cryogenic rolling is required.

#### 4. Summary

In this work, high resolution EBSD was applied to establish the mechanisms of grain refinement during cryogenic rolling of Cu–30%Zn brass. The main conclusions from this work are as follows.

- (1) Cryogenic rolling can be applied to break down millimeter scale grains to produce an ultrafine grain structure. However, the microstructure thus produced tends to be heterogeneous. Broadly speaking, it may be described in terms of texture bands having crystallographic orientations close to the  $\alpha <110>/ND$  fiber and  $\gamma <111>/ND$  fiber. At a local scale, on the other hand, the texture bands contain microstructural features comprising mechanical twins, shear bands, and LABs. Grain refinement was found to be primarily related to twinning and shear banding. The preferential concentration of twins and shear bands within the  $\gamma$  fiber bring about the heterogeneous microstructure.
- (2) The crystallographic orientations of twinned areas are dominated by the  $\gamma$  fiber with a pronounced  $Y \{111\} <112>$  component. The orientation distribution of the shear bands is much broader varying from the  $Y \{111\} <112>$  to Goss  $\{110\} <100>$  and Brass  $\{110\} <112>$  components. This suggests that mechanisms of twinning and shear banding were broadly similar to those occurring during rolling at ambient temperature.

#### Acknowledgments

Financial support from the Russian Fund of Fundamental Research (project No. 14 02 97004) is gratefully acknowledged. The authors are grateful to P. Klassman for technical assistance during cryogenic rolling.

#### References

- [1] Y. Huang, P.B. Prangnell, The effect of cryogenic temperature and change in deformation mode on the limiting grain size in a severely deformed dilute aluminium alloy, *Acta Mater.* 56 (2008) 1619–1632. <http://dx.doi.org/10.1016/j.actamat.2007.12.017>.
- [2] T. Konkova, S. Mironov, A. Korznikov, S.L. Semiatin, Microstructural response of pure copper to cryogenic rolling, *Acta Mater.* 58 (2010) 5262–5273. <http://dx.doi.org/10.1016/j.actamat.2010.05.056>.
- [3] Y.S. Li, N.R. Tao, K. Lu, Microstructural evolution and nanostructure formation in copper during dynamic plastic deformation at cryogenic temperatures, *Acta Mater.* 56 (2008) 230–241. <http://dx.doi.org/10.1016/j.actamat.2007.09.020>.
- [4] Y. Zhang, N.R. Tao, K. Lu, Mechanical properties and rolling behaviors of nano-grained copper with embedded nano-twin bundles, *Acta Mater.* 56 (2008) 2429–2440. <http://dx.doi.org/10.1016/j.actamat.2008.01.030>.
- [5] S.K. Panigrahi, R. Jayaganathan, A study on the mechanical properties of cryorolled Al–Mg–Si alloy, *Mater. Sci. Eng. A* 480 (2008) 299–305. <http://dx.doi.org/10.1016/j.msea.2007.07.024>.
- [6] S.K. Panigrahi, R. Jayaganathan, V. Chawla, Effect of cryorolling on microstructure of Al–Mg–Si alloy, *Mater. Lett.* 62 (2008) 2626–2629. <http://dx.doi.org/10.1016/j.matlet.2008.01.003>.
- [7] V. Subramanya Sarma, J. Wang, W.W. Jian, A. Kauffmann, H. Conrad, J. Freudenberger, Y.T. Zhu, Role of stacking fault energy in strengthening due to cryo-deformation of FCC metals, *Mater. Sci. Eng. A* 527 (2010) 7624–7630. <http://dx.doi.org/10.1016/j.msea.2010.08.015>.
- [8] G.H. Xiao, N.R. Tao, K. Lu, Microstructures and mechanical properties of a Cu–Zn alloy subjected to cryogenic dynamic plastic deformation, *Mater. Sci. Eng. A* 513–514 (2009) 13–21. <http://dx.doi.org/10.1016/j.msea.2009.01.022>.
- [9] S.V. Zharebtsov, G.S. Dyakonov, A.A. Salem, V.I. Sokolenko, G.A. Salishchev, S.L. Semiatin, Formation of nanostructures in commercial-purity titanium via cryo-rolling, *Acta Mater.* 61 (2013) 1167–1178. <http://dx.doi.org/10.1016/j.actamat.2012.10.026>.
- [10] J. Hirsch, K. Lucke, M. Hatherly, Mechanism of deformation and development of rolling textures in polycrystalline F.C.C. metals: III. The influence of slip inhomogeneities and twinning, *Acta Metall.* 36 (1988) 2905–2927. [http://dx.doi.org/10.1016/0001-6160\(88\)90174-5](http://dx.doi.org/10.1016/0001-6160(88)90174-5).
- [11] F.J. Humphreys, Quantitative metallography by electron backscatter diffraction, *J. Microsc.* 195 (1999) 170–185. <http://dx.doi.org/10.1046/j.1365-2818.1999.00578.x>.
- [12] J. Hirsch, K. Lucke, Mechanism of deformation and development of rolling textures in polycrystalline F.C.C. metals: I. Description of rolling texture development in homogeneous CuZn alloys, *Acta Metall.* 36 (1988) 2863–2882. [http://dx.doi.org/10.1016/0001-6160\(88\)90172-1](http://dx.doi.org/10.1016/0001-6160(88)90172-1).
- [13] N. Hansen, D.J. Jensen, Development of microstructure in FCC metals during cold work, *Philos. Trans. R. Soc. Lond. A* 357 (1999) 1447–1469. <http://dx.doi.org/10.1098/rsta.1999.0384>.